# Supplementary materials for:

# Recent acceleration in $N_2O$ growth rate (2013-2023) is caused by increases of nitrogen-fertiliser use and emissions in northern tropics and southern land

*Prabir K. Patra[1,2,3,*], Yasunori Tohjima[4], Akihiko Ito[5], Naveen Chandra[1], Motoki Sasakawa[4], Xin Lan[6,7], Bradley D. Hall[6], Paul B. Krummel[8], Ray F. Weiss[9], Christina M. Harth[9], Shinya Takatsuji[10], Daisuke Goto[11], Kumiko Takata[1], Luke Western[12], Ronald G. Prinn[12]*

1. Research Institute for Global Change, JAMSTEC, Yokohama, 236-0001, Japan

2. Seto Inland Sea Carbon Neutral Research Center, Hiroshima University, Hiroshima 739-8529, Japan

3. Research Institute for Humanity and Nature (RIHN), Kyoto, 603-8047, Japan

4. Earth System Division, National Institute for Environmental Studies (NIES), Tsukuba 305-8506, Japan

5. Graduate School of Agricultural and Life Sciences, The University of Tokyo, Tokyo 113-8657, Japan

6. Global Monitoring Laboratory, National Oceanic & Atmospheric Administration (NOAA), Boulder, CO 80305, USA

7. Cooperative Institute for Research in Environmental Sciences, University of Colorado Boulder, CO 80309, USA

8. CSIRO Environment, Aspendale, Victoria 3195, Australia

9. Scripps Institution of Oceanography, University of California, San Diego, CA 92093, USA

10. Atmospheric Environment and Ocean Division, Atmosphere and Ocean Department, Japan Meteorological Agency (JMA), Tokyo 105-8431, Japan

11. National Institute of Polar Research, Tachikawa, Tokyo, 190-8518, Japan

12. Massachusetts Institute of Technology, Cambridge, MA 02139, USA

* Corresponding author e-mail : prabir@jamstec.go.jp

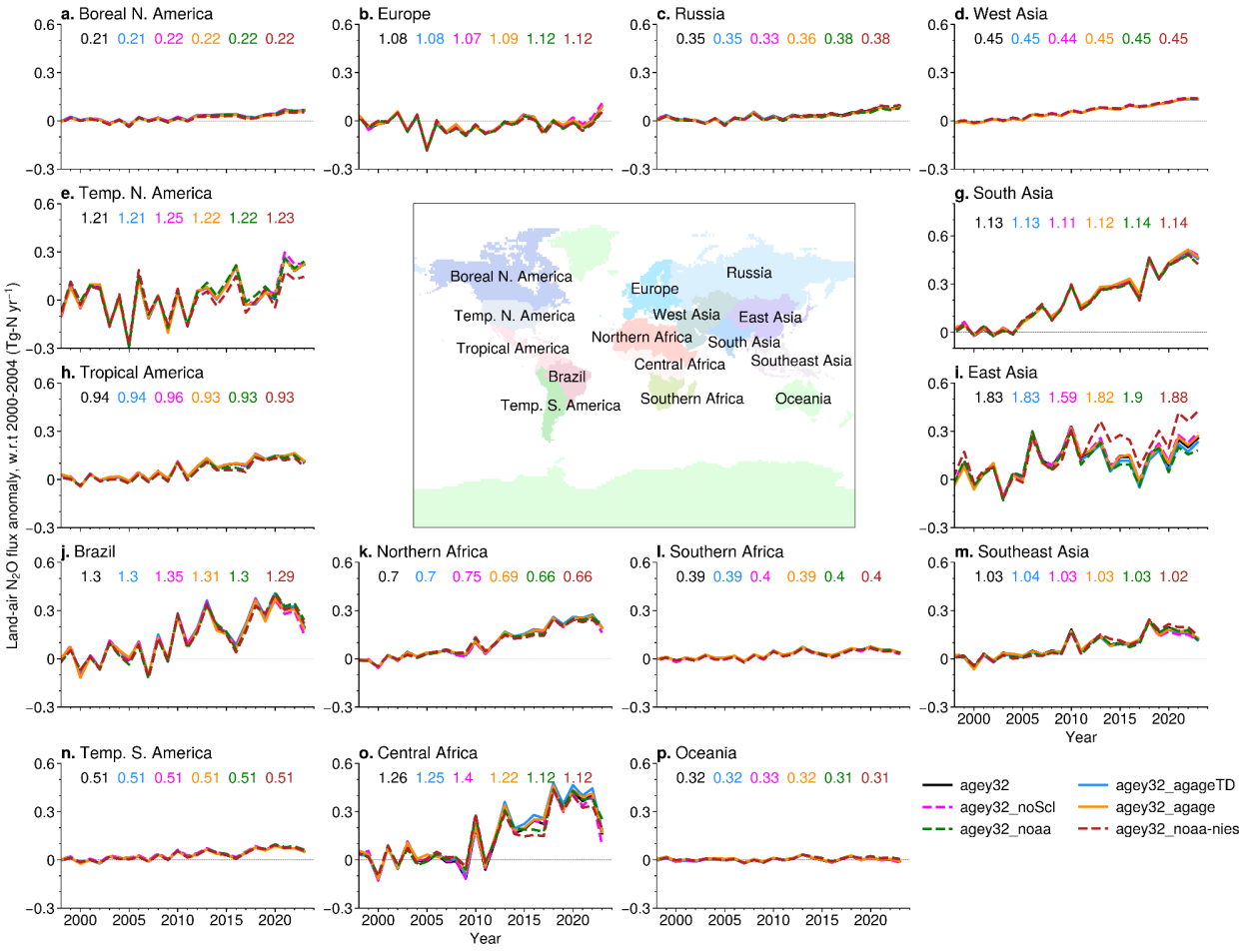


**Figure S1:** Same as Figure 4, but inversions show the effect of NOAA vs AGAGE vs NIES network differences, as well as, the impacts of AGAGE scale selection. The **control case (agey32)** here used all 49 sites data in inversion using "fixed" adjustments for the inter-institional scale differences, while the **case - agey32_agageTD** used the "time-dependent" scale correction to the AGAGE sites, i.e., NOAA/AGAGE = $4.3641 \times 10^{-5}$ * Year + 0.91065 and **case - agey32_noScl** used no scale adjustments. The **case - agey32_agage** excluded 5 NOAA sites (n2o_alt_surface-flask_1, n2o_cgo_surface-flask_1, n2o_mhd_surface-flask_1, n2o_rpb_surface-flask_1, n2o_smo_surface-flask_1), **case - agey32_NOAA** excluded 10 sites of AGAGE and other institute (n2o_alt_surface-flask_16, n2o_brw_surface-insitu_2, n2o_cgo_surface-flask_16, n2o_cgo_surface-insitu_4, n2o_mhd_surface-insitu_4, n2o_mlo_surface-flask_16, n2o_rpb_surface-insitu_4, n2o_smo_surface-insitu_4, n2o_spo_surface-flask_16, n2o_thd_surface-insitu_4), and **case - agey32_NOAA-NIES** excluded 12 sites as in the case of agey32_NOAA + 2 NIES sites (COI_N2O and HAT_N2O). The first 3 cases dealt with measurement scales (49 sites) and final 3 cases show impacts of measurement site networks (fixed scale adjustment).

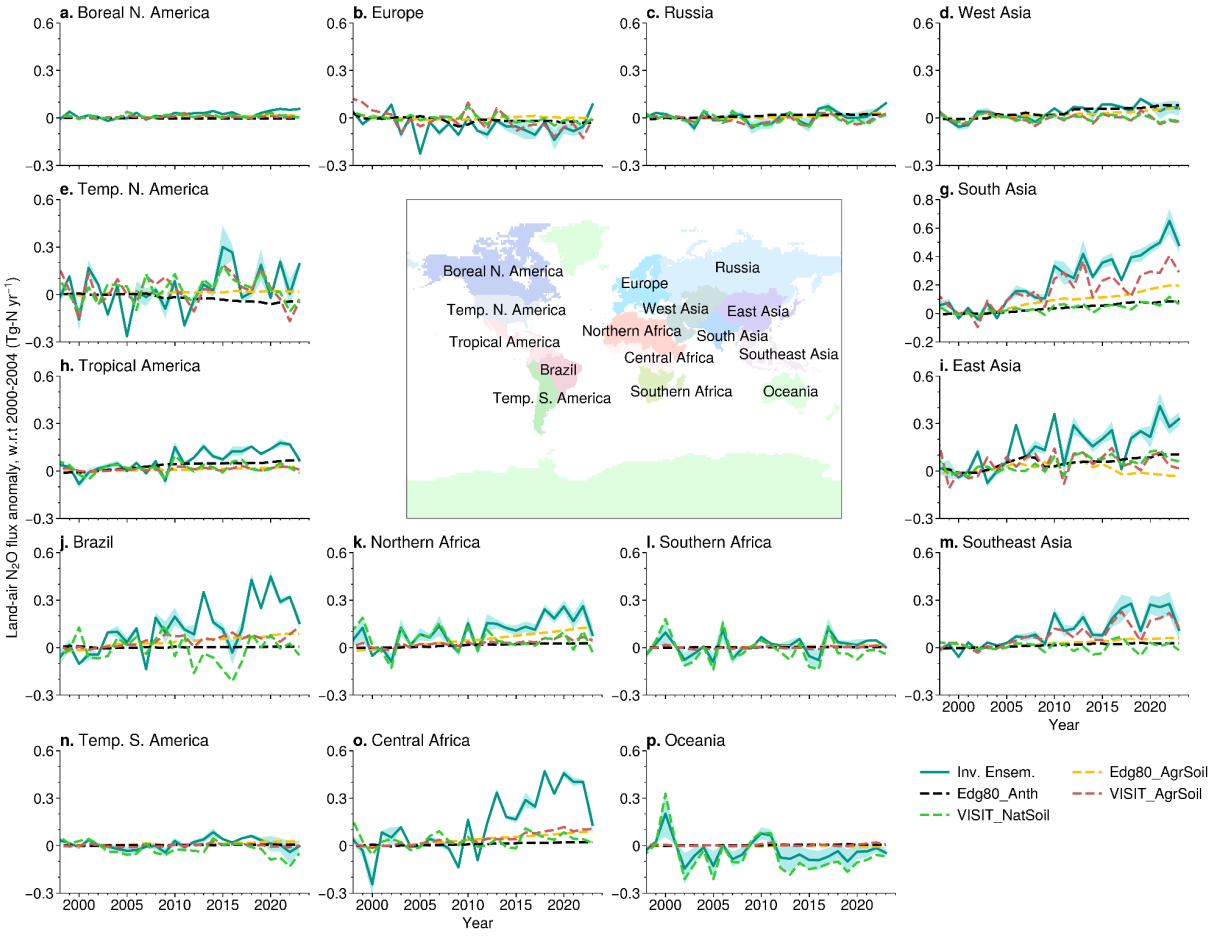


**Figure S2:** Ensemble mean and ±1σ spread (cyan line and shading) of $N_2O$ flux anomalies of 6 inversion cases are shown, and with sectoral fluxes for 4 categories, namely, EDGARv8.0 agriculture soil (Edg80_AgrSoil), EDGARv8.0 anthropogenic/industrial (Edg80_Anth), and VISIT model simulated agriculture soil (VISIT_AgrSoil) and natural soil (VISIT_NatSoil). The GEIA natural soil emissions do not contain interannual variations.

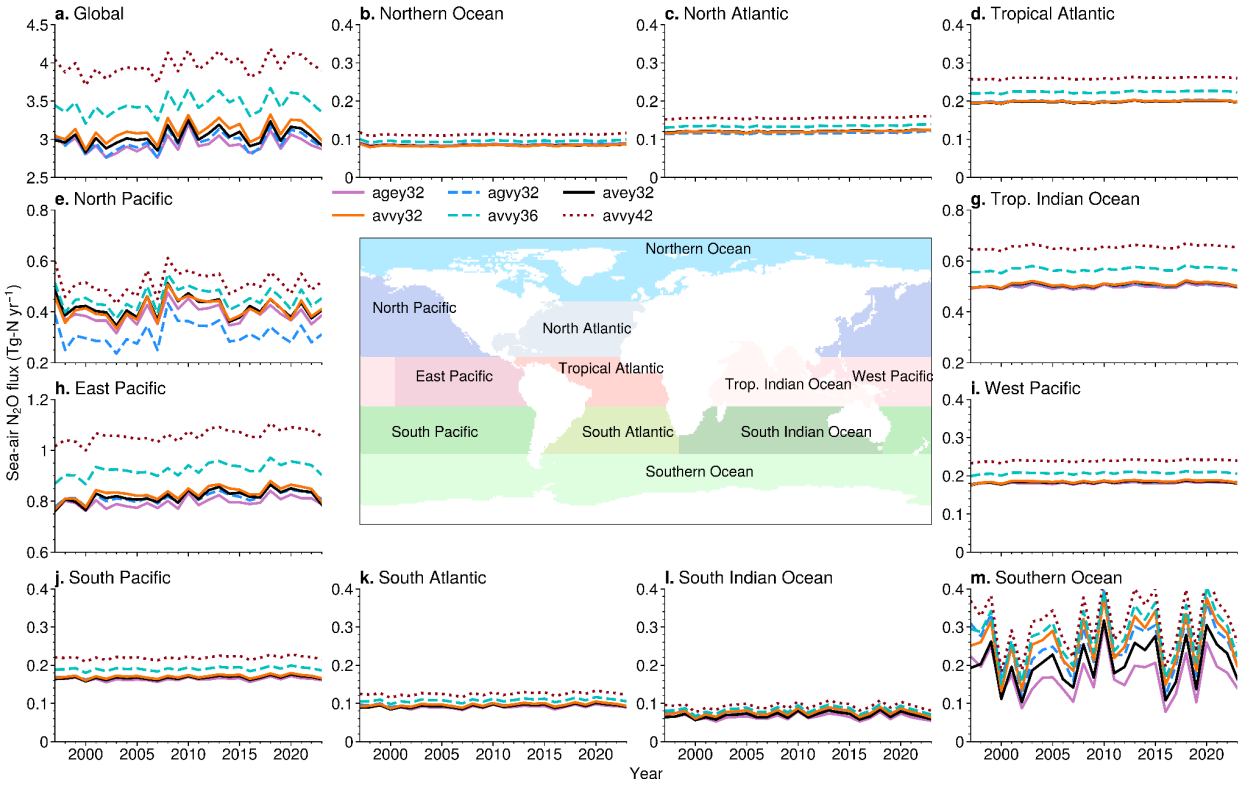


**Figure S3:** Same as Figure 3, but flux time series for the 11 ocean regions are shown.

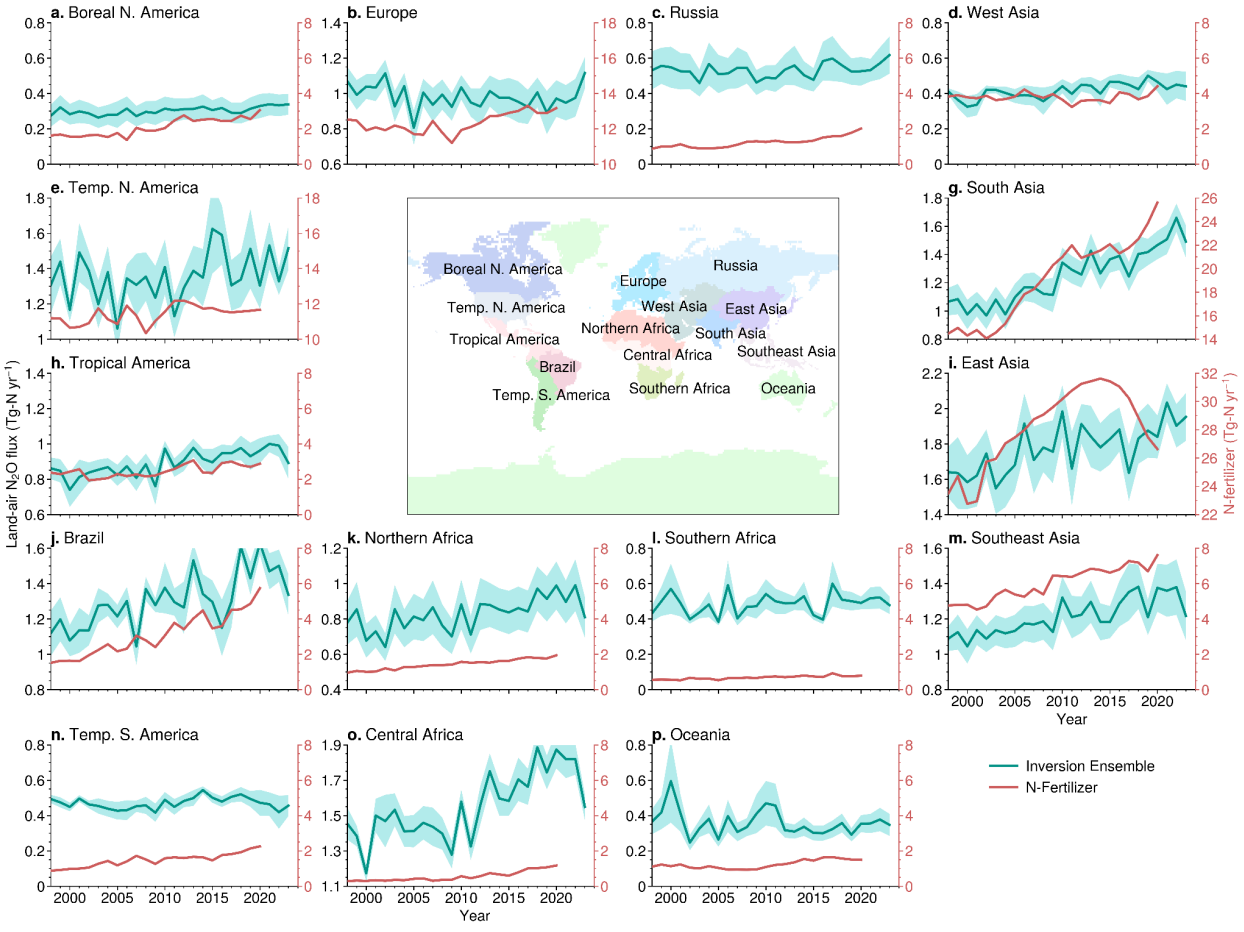


57

58

59 **Figure S4:** Annual mean time series of $N_2O$ total emissions based on ensemble mean and ±1σ
60 spread (cyan line and shading) of different inversion cases for the 15 regions depicted by
61 central map. Nitrogen fertilizer used in the regions are also shown (N-fertilizer = crop_nh4 +
62 crop_no3 + pasture_nh4 + pasture_no3 (red line). The anomalies in ensemble mean and
63 spread between the inversions are shown in Fig. 5 and Fig. S4.


**Figure S5:** Same as Figure S2, but the annual mean anomalies in $N_2O$ flux and ratio of $N_2O$ flux to N-fertilizer use time series are shown. The flux anomalies are calculated relative to the 2000-2004 mean. The N-fertilizer use is assumed to remain constant at 2020 level for the later 3 years.

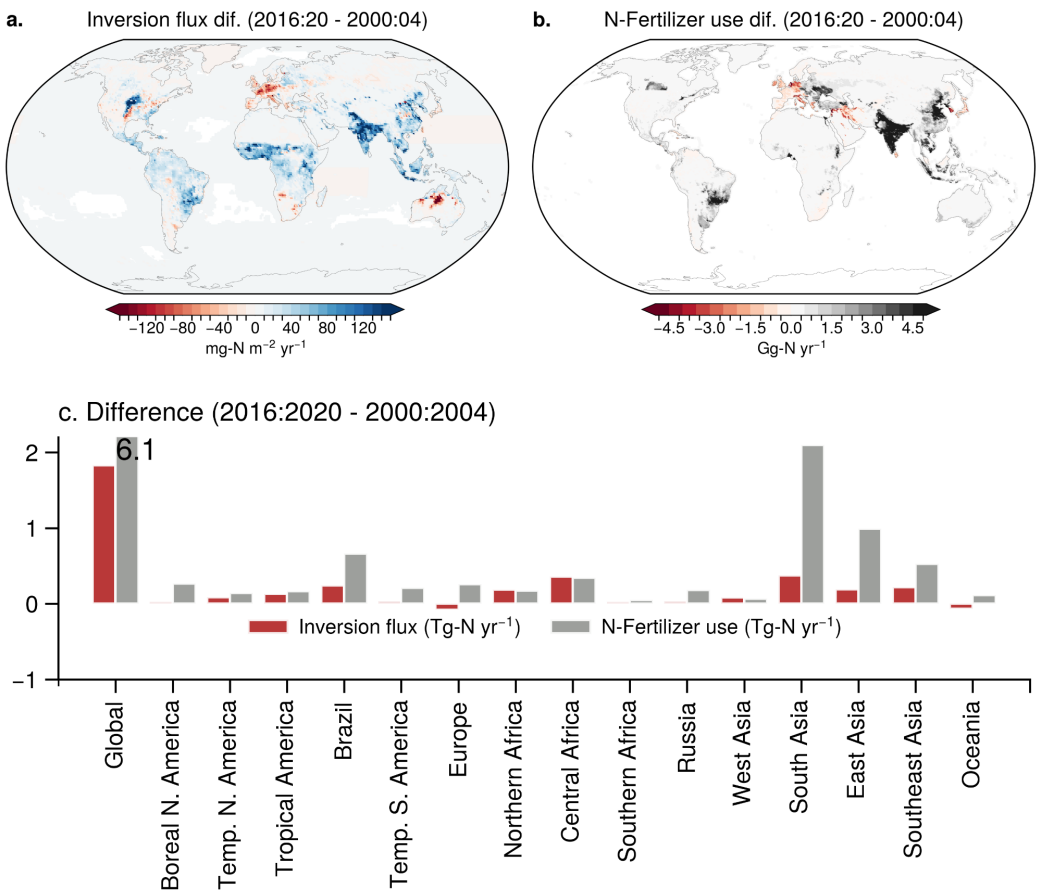


**Figure S6:** Same as Figure 7, but the $N_2O$ flux and N-fertilizer use for the longer period of analysis are shown (2016-2020 and 2000-2004; differences over 16 years). Note that this analysis is restricted until 2020 because of the availability of N-fertilizer input data. Note that the increase in Global N-fertilizer use during the period this analysis is 6.1 as marked on the grey bar and a smaller y-axis range is chosen for clearly showing the regional differences.

**Table S1**. List of sites used in the $N_2O$ inversion as available from NOAA/GML, WDCGG-AGAGE and NIES. Operating institute's name is given at the end of Site name (column 2).

| Sl. No. | Site name and operating institution | Latitude | Longitude | Altitude |
|---|---|---|---|---|
| 1 | n2o_alt_surface-flask_1_NOAA | 82.5 | -62.5 | 190 |
| 2 | n2o_asc_surface-flask_1_NOAA | -8.0 | -14.4 | 90 |
| 3 | n2o_ask_surface-flask_1_NOAA | 23.3 | 5.6 | 2715 |
| 4 | n2o_azr_surface-flask_1_NOAA | 38.8 | -27.4 | 24 |
| 5 | n2o_bmw_surface-flask_1_NOAA | 32.3 | -64.9 | 51 |
| 6 | n2o_brw_surface-flask_1_NOAA | 71.3 | -156.6 | 16 |
| 7 | n2o_cba_surface-flask_1_NOAA | 55.2 | -162.7 | 57 |
| 8 | n2o_cgo_surface-flask_1_NOAA | -40.7 | 144.7 | 164 |
| 9 | n2o_crz_surface-flask_1_NOAA | -46.4 | 51.9 | 202 |
| 10 | n2o_gmi_surface-flask_1_NOAA | 13.4 | 144.7 | 5 |
| 11 | n2o_hba_surface-flask_1_NOAA | -75.6 | -26.2 | 35 |
| 12 | n2o_hun_surface-flask_1_NOAA | 47.0 | 16.7 | 344 |
| 13 | n2o_ice_surface-flask_1_NOAA | 63.4 | -20.3 | 122 |
| 14 | n2o_izo_surface-flask_1_NOAA | 28.3 | -16.5 | 2378 |
| 15 | n2o_key_surface-flask_1_NOAA | 25.7 | -80.2 | 6 |
| 16 | n2o_kum_surface-flask_1_NOAA | 19.6 | -154.9 | 5 |
| 17 | n2o_mhd_surface-flask_1_NOAA | 53.3 | -9.9 | 26 |
| 18 | n2o_mid_surface-flask_1_NOAA | 28.2 | -177.4 | 15 |
| 19 | n2o_mlo_surface-flask_1_NOAA | 19.5 | -155.6 | 3402 |
| 20 | n2o_nwr_surface-flask_1_NOAA | 40.1 | -105.6 | 3526 |
| 21 | n2o_psa_surface-flask_1_NOAA | -64.9 | -64.0 | 15 |
| 22 | n2o_rpb_surface-flask_1_NOAA | 13.2 | -59.4 | 20 |
| 23 | n2o_sey_surface-flask_1_NOAA | -4.7 | 55.5 | 7 |
| 24 | n2o_shm_surface-flask_1_NOAA | 52.7 | 174.1 | 28 |
| 25 | n2o_smo_surface-flask_1_NOAA | -14.3 | -170.6 | 60 |
| 26 | n2o_spo_surface-flask_1_NOAA | -89.0 | -24.8 | 2815 |
| 27 | n2o_syo_surface-flask_1_NOAA | -69.0 | 39.6 | 19 |
| 28 | n2o_tap_surface-flask_1_NOAA | 36.7 | 126.1 | 21 |
| 29 | n2o_ush_surface-flask_1_NOAA | -54.9 | -68.3 | 32 |
| 30 | n2o_uta_surface-flask_1_NOAA | 39.9 | -113.7 | 1332 |
| 31 | n2o_uum_surface-flask_1_NOAA | 44.5 | 111.1 | 1012 |
| 32 | n2o_wis_surface-flask_1_NOAA | 30.0 | 35.1 | 156 |
| 33 | n2o_zep_surface-flask_1_NOAA | 78.9 | 11.9 | 479 |
| 34 | n2o_brw_surface-insitu_2_NOAA | 71.3 | -156.6 | 16 |
| 35 | n2o_cgo_surface-insitu_4_AGAGE | -40.7 | 144.7 | 164 |
| 36 | n2o_mhd_surface-insitu_4_AGAGE | 53.3 | -9.9 | 8 |
| 37 | n2o_rpb_surface-insitu_4_AGAGE | 13.2 | -59.4 | 20 |
| 38 | n2o_smo_surface-insitu_4_AGAGE | -14.2 | -170.6 | 60 |
| 39 | n2o_thd_surface-insitu_4_AGAGE | 41.1 | -124.2 | 2 |
| 40 | n2o_alt_surface-flask_16_CSIRO | 82.5 | -62.3 | 210 |
| 41 | n2o_cgo_surface-flask_16_CSIRO | -40.7 | 144.7 | 164 |
| 42 | n2o_cya_surface-flask_16_CSIRO | -66.3 | 110.5 | 55 |
| 43 | n2o_maa_surface-flask_16_CSIRO | -67.6 | 62.9 | 42 |
| 44 | n2o_mlo_surface-flask_16_CSIRO | 19.5 | -155.6 | 3435 |
| 45 | n2o_mqa_surface-flask_16_CSIRO | -54.5 | 158.9 | 13 |
| 46 | n2o_spo_surface-flask_16_CSIRO | -89.0 | -24.8 | 2847 |
| 47 | n2o_ryo_surface-insitu_1_JMA | 39.0 | 141.8 | 280 |
| 48 | n2o_coi_surface-insitu_NIES | 43.2 | 145.5 | 101 |
| 49 | n2o_hat_surface-insitu_NIES | 24.1 | 123.8 | 47 |